

Dynamic Solid-State NMR Experiments Reveal Structural Changes for a Methyl Silicate Nanostructure on Deuterium Substitution

Hans J. Jakobsen,^{*,†} Anders T. Lindhardt,[‡] Henrik Bildsøe,[†] Jørgen Skibsted,[†] Zhehong Gan,[§] Ivan Hung,[§] and Flemming H. Larsen^{||}

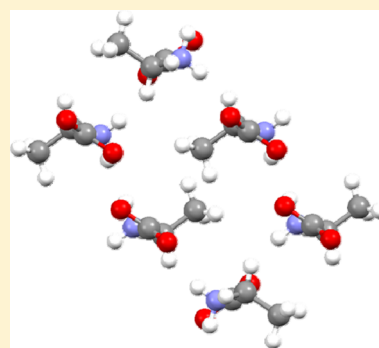
[†]Department of Chemistry, Interdisciplinary Nanoscience Center (iNANO), and [‡]Department of Engineering, Interdisciplinary Nanoscience Center (iNANO), Aarhus University, DK-8000 Aarhus C, Denmark

[§]National High Magnetic Field Laboratory, 1860 East Paul Dirac Drive, Tallahassee, Florida 32310, United States

^{||}Department of Food Science, University of Copenhagen, DK-1958 Frederiksberg C, Denmark

Supporting Information

ABSTRACT: Structural characterizations of three different solid–gas reaction products, recently obtained from abraded solid-state silicate free radicals reacting with two isotopically enriched methane gases, $^{13}\text{CH}_4$ and CD_4 (a possible sink for methane on MARS) and with $^{13}\text{CO}_2$, are derived from various dynamic solid-state NMR experiments. These include cross-polarization/depolarization zero-cross times (ZCTs), variable temperature (VT) NMR to study 3-site jump CH_3/CD_3 activation energies (E_a), and $^{13}\text{CO}_2/^{13}\text{CH}_3$ molecular species as a spy to determine the approximate diameters for the channel structures for some of these structures. Literature E_a data indicate that L-alanine and 4- CH_3 -phenanthrene exhibit the highest known E_a values ($= 20\text{--}22.6$ kJ/mol) for CH_3 3-site jump motions. The ZCTs for these two compounds are 120 and 162 μs , respectively, indicative of the high E_a values for CH_3/CD_3 groups. Determination of E_a for 4- CD_3 -phenanthrene by low-temperature ^2H MAS NMR experiments supplemented the previously reported liquid-state E_a value ($E_a = 21$ kJ/mol) for 4- CH_3 -phenanthrene. Finally, such experiments also revealed the structural difference for the free-radical reaction products with $^{13}\text{CH}_4$ and CD_4 , i.e., a change from helical to chain structure.



INTRODUCTION

A recent solid-state NMR and EPR investigation reveals that a special created silicate free-radical intermediate undergoes a new kind of solid–gas chemical reaction with some ordinary gases.¹ In particular, among these ordinary gases, its reaction with methane (isotopically enriched $^{13}\text{CH}_4$ and CD_4) is until now the most intensively studied gas reaction.¹ The solid-state Si free-radical intermediate and its gas-reaction silicate products are formed in a newly designed, slow-rotating apparatus which by mechanical tumbling of Pyrex glass flasks (containing abrasive particles and gases) mimics the winds and collision speed of the mineral particles on Mars.^{1,2} These recent NMR and EPR results¹ prove that abrasive effects of hard materials (e.g., $\text{SiO}_2/\text{quartz}$ or $\alpha\text{-Al}_2\text{O}_3/\text{corundum}$ grains) on softer Si-containing glasses (e.g., Pyrex and quartz glasses) produce free radicals with unpaired electrons residing on the silicon atoms. In addition, our recent EPR results¹ also show that these free radicals are identical to the proposed free-radical submicroscopic silicate structure (today named “silicate nanomaterial”) observed from γ -irradiation of Pyrex and quartz glasses,^{3–10} however, of unknown chemical structure. Ever since these very early EPR proposals of either small chains or helices for the structure of the free radical silicate nanomaterial,^{3–10} apparently no new conclusive structural information has been obtained for the radical or for the gas reaction products, as produced and

recently investigated.¹ The many years of ongoing dispute among Mars researchers on the reasons for the apparently rapid disappearance and reappearance of methane on Mars¹ (e.g., at the Gale crater by the Curiosity team^{11,12}) has provoked an intense solid-state NMR structural investigation by our solid-state NMR group on the reaction products following reaction of the radical (or possibly through further intermediate stages) with methane. From this kind of silicate free radical intermediate and its reaction products with methane and other gases, created from our terrestrial experimental simulations of the Mars wind erosion on its mineral, a possible sink for methane on Mars could recently be proposed.¹

To obtain additional information and insight into the structure of the free radical silicate nanomaterial and its reaction products, we have undertaken new terrestrial solid-state NMR experiments. Here we report solid-state room-temperature (RT) MAS and very low variable-temperature (VT) MAS NMR dynamic experimental results on the methane reaction products for the two isotopic $^{13}\text{CH}_4$ and CD_4 gases, recently isolated in small quantities (~ 100 mg) following sieving to enhance their solid concentrations¹ and labeled (1)

Received: September 6, 2017

Revised: November 2, 2017

Published: November 3, 2017

and (2), respectively, in the present study. The solid-state RT data are obtained from an array of $^{13}\text{C}\{^1\text{H}\}$ cross-polarization–depolarization (CP/DP) MAS experiments for the $^{13}\text{CH}_4$ reaction product (1), which has been shown to contain both one-bond $^{13}\text{CH}_3\text{—Si}\equiv$ and $\text{HO—Si}\equiv$ covalent bonds.^{1,2} Originally the CP/DP experiment was introduced by Melchior¹³ and further developed into a tool for ^{13}C MAS spectral editing of organic solids.^{14,15} In the present work the CP/DP experiments are performed (i) to obtain a precise value for the very short $^{13}\text{CH}_3$ zero-cross time (ZCT) indicated earlier for this $^{13}\text{CH}_3\text{—Si}\equiv$ group² and (ii) for comparison with precise ZCTs, determined here for the first time for $^{13}\text{CH}_3$ groups known to reside in highly congested CH_3/CD_3 environments.^{16–19} The earlier observed congested CH_3/CD_3 environments have been investigated using other type of $^1\text{H}/^{13}\text{C}/^2\text{H}$ VT dynamic experiments.^{17–19} Therefore, our $^{13}\text{C}\{^1\text{H}\}$ CP/DP experiments include precise experimental ZCT data for the CH_3 groups in L-alanine (L- $\text{CH}_3\text{CH}(\text{NH}_2)\text{—COOH}$) (7) and 4- CH_3 -phenanthrene (4) because these two materials contain some of the most constrained CH_3 -group rotational barriers with determined activation energies E_a of 22.6 kJ/mol¹⁷ and 20.0 kJ/mol¹⁹ for CD_3 -L-alanine (L-[3,3,3- D_3]alanine) (8) and $E_a = 21.1$ kJ/mol for 4- CH_3 -phenanthrene (4).¹⁸

The E_a values of 22.6 and 20.0 kJ mol⁻¹ for CD_3 -L-alanine (8) were determined from low-temperature solid-state VT ^2H static NMR spin–lattice relaxation study¹⁷ and line-shape analysis,¹⁹ respectively, while the value $E_a = 21.1$ kJ/mol for 4- CH_3 -phenanthrene (4)¹⁸ was obtained from VT ^1H spin–lattice relaxation time (T_1) measurements using a degassed liquid-state sample. To complement and compare this latter E_a value determined from the liquid-state ^1H NMR measurements with the static solid-state VT ^2H NMR results for CD_3 -L-alanine (8),^{17,19} we have in addition to the CP/DP investigations performed solid-state VT ^2H dynamic experiments, which employ MAS as opposed to static NMR. These investigations are performed on (iii) the CD_3 group for a synthesized deuterated sample of 4- CD_3 -phenanthrene (5) and (iv) for the one-bond $\text{CD}_3\text{—Si}\equiv$ species of the CD_4 reaction product (2).¹ The theoretical calculations and extractions of the dynamic parameters (E_a and A frequency factors) from low-temperature VT ^2H MAS NMR experimental spectra have in recent years been intensively investigated and reviewed by Larsen.^{20,21} To our knowledge the present low-temperature VT ^2H MAS NMR experiments are the first VT ^2H MAS NMR experiments supporting Larsen's theoretical simulations^{20,21} of the rotational 3-site jump process for CD_3 group dynamics. At this point we note that the advantages of the dynamic VT MAS vs VT static NMR are large savings in spectrometer time, similar to the well-known sensitivity enhancements obtained by QCPMG^{20,22,23} experiments in static NMR of quadrupolar nuclei in solids. Considering the extremely long ^2H T_1 relaxation times encountered at the low temperatures of -170 to -150 °C for the ~ 40 mg sample of 4- CD_3 -phenanthrene (5) in a 3.2 mm rotor, we note that the VT ^2H MAS dynamic results reported here would have been impossible to obtain without access to either very low-temperature VT QCPMG static or MAS instrumentation. The extreme increase in $T_1(^2\text{H})$ relaxation times appears to be a characteristic feature for CD_3 group 3-site jumps in the slow regime $k(\text{CD}_3) \ll C_Q$ as observed here for temperatures < -150 °C. Such huge increases in $T_1(^2\text{H})$ relaxation times have

also recently been observed/investigated for protein CD_3 groups at the lower temperatures of ~ 90 K (~ -183 °C) and for lower E_a values^{24,25} compared to the congested methyl groups studied here.

Finally, we have taken further advantage of our recent RT ^{13}C MAS NMR study of the reaction product (named (3)) resulting from reaction between the recently produced silicate free-radical intermediate¹ and ^{13}C -enriched $^{13}\text{CO}_2$ gas, which shows that the CO_2 molecules get encapsulated within the silicate structure.¹ Thus, here we use the $^{13}\text{CO}_2$ molecule as a spy or molecular probe to obtain additional information on this structure following two recent reports^{26,27} on CO_2 molecules confined in the micropores of solids.

EXPERIMENTAL SECTION

Materials and Synthesis. The preparation, isolation including different steps of sieving, and finally characterization of the two solid–gas reaction products obtained from the solid-state free-radical silicate nanomaterial and the two isotopically enriched $^{13}\text{CH}_4$ and CD_4 methane gases are described in detail in a recent article.¹ Characterizations of the reaction product with enriched $^{13}\text{CH}_4$, i.e., sample 1 ($^{13}\text{CH}_4$ -tumbled SiO_2 grains–Simax flask; sieved (< 100 μm) and handled in open air), are described and shown in the RT ^{13}C and ^{29}Si MAS NMR spectra of Figures 2 and 4, respectively, in ref 1. Similarly, the characterizations of the reaction product with ^2H -enriched CD_4 gas, i.e., in the present article named sample (2) (CD_4 -tumbled SiO_2 grains–Simax flask; sieved (< 100 μm) and handled in open air), are described and shown in the RT ^2H MAS NMR spectra of Figure 6 in ref 1. A final sample prepared and partly studied earlier¹ is the reaction product involving $^{13}\text{CO}_2$ gas, i.e., in the present article named sample (3) ($^{13}\text{CO}_2$ -tumbled SiO_2 grains–Simax flask; sieved (< 250 μm) and handled in open air), as described and shown in the RT ^{13}C MAS NMR spectra of Figure 9 in ref 1. Two new samples investigated in the present study, 4- CH_3 -phenanthrene (4) and 4- CD_3 -phenanthrene (5), were also synthesized in our laboratories. These samples both used a commercially available compound, 2,3-dihydro-1H-phenanthrene-4-one from Gute Chemie, ABCR, Germany, as starting material for the synthesis of these compounds from Grignard reactions employing ethereal solutions of CH_3MgI and CD_3MgI , respectively, commercially available from Sigma-Aldrich. The synthesis of 4- CH_3 -phenanthrene (4) (Grignard, H_3O^+ water elimination, Pd/C final aromatization, and recrystallization from alcohol) following all its steps resulted in an 80% yield of pure 4- CH_3 -phenanthrene (mp $49\text{--}50$ °C; literature $48\text{--}49$ °C). However, beforehand, we expected the synthesis of 4- CD_3 -phenanthrene (5) to cause deuterium (D) scrambling introduced by the carbonium ion (following the $\text{H}_3\text{O}^+/\text{H}_2\text{DO}^+$ water elimination process using *p*-toluenesulfonic acid) in both the aromatic ring and the CD_3 side-chain structure. Indeed, this was observed to be the case because the sample was shown to constitute a mixture of $\sim 50\%$ of 4- CD_3 -phenanthrene (5) and $\sim 50\%$ of 4- $\text{CD}_2\text{H-3D}$ -phenanthrene (6) using a combination of high-field liquid-state ^{13}C and ^1H NMR. An evaluation of this interesting deuterium scrambling process for these two deuterium isotopomers is presently being investigated in detail in a separate liquid-state ^{13}C NMR study. This liquid-state study involves observation of magnetic field alignments for these two specially deuterated aromatic molecules in magnetic field strengths ranging from 2.35 to 22.33 T, including the various

D-isotope effects (on ^{13}C chemical shifts and $^nJ(^{13}\text{C}-^1\text{H})$ coupling constants) and residual dipolar couplings to assist in the assignments of the ^{13}C resonances introduced by the quite similar magnetic field alignments for the two isotopomers.

The only remaining compounds referred to or used in this study are L-alanine (7), CD_3 -L-alanine (8), hexamethylbenzene (HMB) (9), and sodium 3-trimethylsilylpropylsulfonate (10) (often referred to as the “solid-state TMS-salt”) which are all commercially available.

Solid-State MAS NMR Spectroscopy. The RT $^{13}\text{C}\{^1\text{H}\}$ CP/DP MAS NMR experiments were performed at Aarhus University on a Varian INOVA-300 narrow-bore 7.05 T spectrometer operating at 75.43 MHz for ^{13}C using a home-built 5 mm CP/MAS probe, 5 mm o.d. zirconia rotors ($\sim 110\ \mu\text{L}$ sample volume), and a spinning frequency $\nu_r = 3.0\ \text{kHz}$ for all samples investigated using our original CP/DP pulse sequence.¹⁵ All $^{13}\text{C}\{^1\text{H}\}$ CP/DP MAS NMR experiments used ^{13}C and ^1H rf field strengths of $\gamma B_1/2\pi \approx \gamma B_2/2\pi = 60\ \text{kHz}$ during the CP and DP contact times, $\gamma B_2/2\pi = 100\ \text{kHz}$ for the initial $90^\circ\ ^1\text{H}$ pulse and ^1H TPPM decoupling, and a relaxation delay of 4 s. The CP contact times were optimized for each individual sample and were all in the range 500–5000 μs (see the figure captions and the Supporting Information). The number of scans acquired for each array value within the CP/DP experiments for the individual samples very much depended on the CH_3 group concentrations within the samples and varies from 16 to 2048 scans as indicated in the figure captions for the spectra along with the optimized contact times.

The series of low-temperature VT ^2H MAS NMR spectra (i) for the solid 1:1 mixture (*vide supra*) of 4- CD_3 -phenanthrene (5) and 4- CD_2H -3D-phenanthrene (6) and (ii) for the one-bond CD_3 -Si \equiv units of the CD_4 reaction product (2) with the silicate free radical were performed at the National High Magnetic Field Laboratory (NHMFL, the MagLab) in Tallahassee, FL. These ^2H MAS experiments were performed on a Bruker prototype DNP 600 MHz (14.10 T) wide-bore spectrometer (Avance-III) operating at 92.12 MHz for ^2H (and without using DNP). The spectrometer was equipped with a prototype Bruker low-temperature DNP $\text{X}\{^1\text{H}\}$ double-resonance MAS probe which incorporates a VT stator for 3.2 mm rotors. Three separate N_2 gas cooling lines are connected to the stator (for air-bearing, air-drive, and sample-cooling), with the temperature and flow of the gas in each line being individually under computer control in order to achieve the lowest possible temperature and highest stability using N_2 cooling gas. Employing this VT MAS probe setup allows MAS experiments for $\nu_r < 8\ \text{kHz}$ to be performed in the temperature range from about $-180\ ^\circ\text{C}$ and up close to $-10\ ^\circ\text{C}$. A most impressive and noticeable effect of this VT stator design is that temperature calibration of the actual MAS sample temperatures, using the standard $\text{Pb}(\text{NO}_3)_2$ method,²⁸ shows that these temperatures are very much identical to the read-out temperatures in the sample-cooling line, even for the lowest temperatures obtainable for this MAS probe, and with a precision in temperatures $\Delta T = \pm 2\ ^\circ\text{C}$. The VT range employed in the ^2H MAS study for the 4- CD_3 -phenanthrene sample (i, 5/6) and the CD_3 -Si \equiv /DO-Si \equiv sample (ii, 2) described above is -170 to $-30\ ^\circ\text{C}$, with the first experiment performed always being the one at lowest temperature ($-170\ ^\circ\text{C}$) after full temperature stabilization of the probe at this temperature. The MAS frequency for sample (i, 5/6) is $\nu_r = 6.0\ \text{kHz}$ and for (ii, 2) $\nu_r = 2.0\ \text{kHz}$ (with a stability $\Delta\nu_r < \pm 1\ \text{Hz}$).

All ^2H MAS spectra were acquired using single-pulse excitation. A 90° flip-angle $\text{pw}(90)_{\text{liquid}} = 6.0\ \mu\text{s}$ was obtained for the ^2H resonance of D_2O while a value of $\text{pw} = 2.0\ \mu\text{s}$, which corresponds to a liquid 30° flip angle, was used for the MAS experiments. Because an extremely long T_1 spin–lattice relaxation time (not determined, *vide supra*) was observed for at least the lowest temperature of $-170\ ^\circ\text{C}$ for sample (i, 5/6), a relaxation delay of 10 s was used for the temperatures of -170 and $-150\ ^\circ\text{C}$ but was gradually lowered to 2, 0.5, and finally 0.1 s for the higher temperatures. However, in contrast, for sample (ii, 2) a relaxation delay of only 0.1 s could be used even at the lowest temperature ($-170\ ^\circ\text{C}$). Because of the extremely long T_1 observed for (i, 5/6) at the lowest temperature, the number of scans required to obtain decent S/N ratios could be decreased for this sample from 8192 to 2048 with an increase in the temperature range from >-150 to $-30\ ^\circ\text{C}$. ^2H chemical shifts are relative to neat TMS (^1H) using a neat sample of CDCl_3 and $\delta_{\text{iso}}(^2\text{H}) = \delta_{\text{iso}}(^1\text{H}) = 7.27\ \text{ppm}$ as secondary references. While the ^2H chemical shifts (δ_{iso}) have a precision of about $\pm 0.5\ \text{ppm}$, the precision of the ^2H chemical shift differences between the two groups of resonances for sample (i, 5/6) is only about $\pm 0.1\ \text{ppm}$.

Solid-State NMR Spectral Analysis. Analysis of the ^2H MAS NMR spectra was performed employing the STARS software package²⁹ and the upgraded version also used and described in a recent article.¹

The quadrupole coupling and CSA parameters are defined by

$$C_Q = eQV_{zz}/h \quad \eta_Q = (V_{yy} - V_{xx})/V_{zz} \quad (1)$$

$$\delta_\sigma = \delta_{\text{iso}} - \delta_{zz} \quad \eta_\sigma = (\delta_{xx} - \delta_{yy})/\delta_\sigma \quad (2)$$

$$\delta_{\text{iso}} = (1/3)(\delta_{xx} + \delta_{yy} + \delta_{zz}) = (1/3)\text{Tr}(\delta) \quad (3)$$

using the convention

$$|\lambda_{zz} - (1/3)\text{Tr}(\lambda)| \geq |\lambda_{xx} - (1/3)\text{Tr}(\lambda)| \geq |\lambda_{yy} - (1/3)\text{Tr}(\lambda)| \quad (4)$$

for the principal elements ($\lambda_{aa} = V_{aa} \delta_{aa}$) of the two tensors. The relative orientation of the two tensors is described by the three Euler angles (ψ , χ , ξ) which correspond to positive rotations of the CSA principal axis system around $z(\psi)$, the new $y(\chi)$, and the final $z(\xi)$ axis.

The extraction of the rate constants from the different low-temperature VT ^2H MAS NMR spectra was performed by analysis using the software package (slightly modified) developed and reviewed by Larsen for simulation of molecular motion of quadrupolar nuclei in solid-state NMR.^{20,21} Using this software, the “ $\text{CD}_3/\text{CD}_2\text{H}$ -only” spectra recorded at different temperatures were simulated following subtraction of the ^2H MAS spectrum for the aromatic deuterium in position 3 (*vide infra*). The simulations employed fixed C_Q and η_Q parameters as well as the angle (named β_{PC}) between the C–D bond and the 3-fold axis and only varying the rate constant for the 3-site jump process for the spectra recorded at the different temperatures. These rate constants were subsequently used for determination of the activation energy for the 3-site jump process using the Arrhenius equation.

RESULTS AND DISCUSSION

Solid-State $^{13}\text{C}\{^1\text{H}\}$ Cross-Polarization/Depolarization (CP/DP) MAS Studies of Congested CH_3 Groups. For Melchior’s original CP/DP experiment,¹³ theoretical optimized

spectral editing conditions¹⁵ and experiments^{14,15} for the different types of $^{13}\text{C}_n\text{H}_n$ groups ($n = 3, 2, 1, 0$) show that their intensities may vary widely according to the number n of H_n hydrogens within the $^{13}\text{C}_n\text{H}_n$ group and the dynamics of these groups. For example, for rapid rotational 3-site jumps of standard CH_3 groups residing in noncongested environments and for quaternary carbons, their carbon resonances are unable to zero-cross within the DP times ($< \sim 600 \mu\text{s}$) usually employed in spectral editing of CH_n ($n = 3, 2, 1, 0$) carbon resonances. Generally, the zero-cross times (ZCTs) for CH_n groups are $n = 2$: $\sim 20\text{--}30 \mu\text{s}$; $n = 1$: $\sim 30\text{--}40 \mu\text{s}$; $n = 3$: $> 600 \mu\text{s}$ (mobile CH_3 groups) or not observed, and finally for $n = 0$: not observed. To obtain an improved interrelationship between the ZCTs for the congested CH_3 groups studied in this research and the activation energies E_a determined for other CH_3 groups, we here refer to the following list of compounds, E_a values, literature references, which have been summarized by Griffin and co-workers¹⁹ in their study on CD_3 dynamics in CD_3 -L-alanine (8) resulting in a value $E_a = 20.0 \text{ kJ/mol}$. Note: the literature references shown here are those listed in the article by Griffin and co-workers:¹⁹ other amino acids, $E_a = 8\text{--}17 \text{ kJ/mol}$, refs 10, 19, 20, and 22; CH_3 groups in *tert*-butyl compounds, $E_a = 6\text{--}12 \text{ kJ/mol}$, ref 24; CH_3 groups substituted in aromatic hydrocarbons, $E_a = 9\text{--}11 \text{ kJ/mol}$, ref 25. Thus, the value $E_a = 21.1 \text{ kJ/mol}$ obtained for 4- CH_3 -phenanthrene (4) employing ^1H relaxation studies¹⁸ is just slightly higher than the value determined by Griffin and co-workers for CD_3 -L-alanine (8)¹⁹ but slightly lower than the value determined by Batchfelder et al.¹⁷

Considering the ZCTs generally observed for different CH_n groups (*vide supra*), it was somewhat of a surprise to observe the extremely short ZCT of $120 \pm 3 \mu\text{s}$ determined from the $^{13}\text{C}\{^1\text{H}\}$ CP/DP MAS NMR experiments in Figure 1 for the one-bond $^{13}\text{CH}_3\text{--Si}\equiv$ methyl group of the fully protonated reaction product (1) obtained from the reaction with $^{13}\text{CH}_4$.¹ This observation inspired us to explore if CP/DP experiments for the two published highly congested CH_3 groups, i.e., from

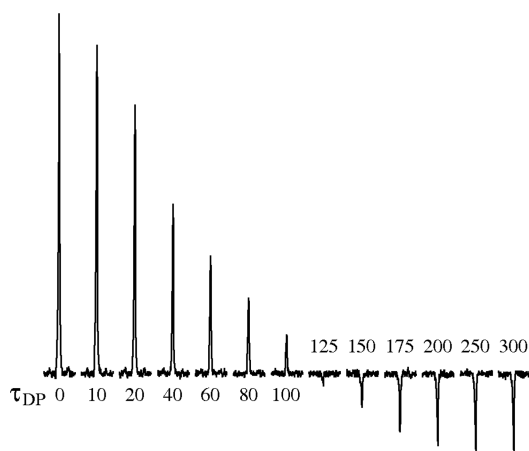


Figure 1. $^{13}\text{C}\{^1\text{H}\}$ cross-polarization/depolarization (CP/DP) MAS experiments for the one-bond $^{13}\text{CH}_3\text{--Si}\equiv$ methyl group of the reaction product (1) obtained from reaction with $^{13}\text{CH}_4$.¹ The sample (1) contains $\text{CH}_3\text{--}^{29}\text{Si}\equiv$ and $\text{HO--}^{29}\text{Si}\equiv$ groups and has been sieved using a $250 \mu\text{m}$ sieve. Each of the 13 CP/DP experiments is labeled with the employed depolarization time (τ_{DP}) in μs , used 2048 scans, a CP contact time of $900 \mu\text{s}$, a MAS frequency $\nu_r = 3.0 \text{ kHz}$, and a relaxation delay of 4.0 s . The zero-cross time (ZCT) time for the $^{13}\text{CH}_3\text{--Si}\equiv$ methyl group is seen to be $120 \pm 3 \mu\text{s}$.

the precise neutron diffraction crystal and molecular structure of L-alanine (7)¹⁶ and CD_3 dynamics in CD_3 -L-alanine (8),^{17,19} along with the E_a value for 4- CH_3 -phenanthrene (4)¹⁸ (*vide supra*), would result in values being in accordance with the short ZCT ($120 \pm 3 \mu\text{s}$) determined above for (1).

The series of $^{13}\text{C}\{^1\text{H}\}$ CP/DP MAS NMR experiments performed for the CH_3 group in a polycrystalline sample of L-alanine (7) are illustrated in Figure 2 and show a ZCT of $120 \pm$

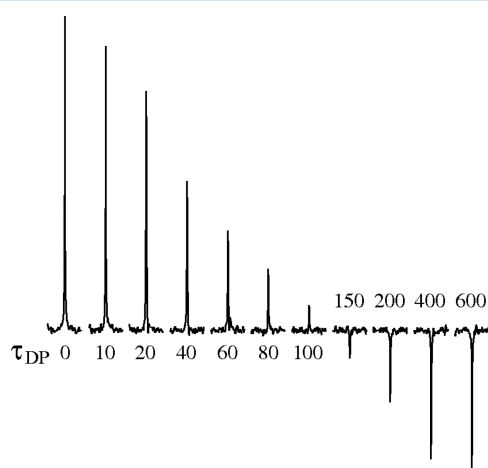


Figure 2. $^{13}\text{C}\{^1\text{H}\}$ CP/DP MAS experiments for the CH_3 group in L-alanine (7). Each of the CP/DP experiments used 16 scans, a CP contact time of $500 \mu\text{s}$, a relaxation delay of 4.0 s , and a MAS frequency of $\nu_r = 3.0 \text{ kHz}$. The DP time (τ_{DP}) shown below/above each spectrum is in μs . The ZCT for the CH_3 group is observed at $125 \pm 5 \mu\text{s}$.

$5 \mu\text{s}$, exactly identical to that determined for sample (1). For 4- CH_3 -phenanthrene (4) the $^{13}\text{C}\{^1\text{H}\}$ CP/DP MAS spectra for the CH_3 group are displayed in Figure 3 and show a ZCT of $162 \pm 5 \mu\text{s}$, i.e., a little longer as observed for the $^{13}\text{CH}_3\text{--Si}\equiv$ units in the reaction product (1) with $^{13}\text{CH}_4$ and for L-alanine (7), but still characteristic for a highly constrained CH_3 group. The somewhat longer ZCT observed for 4- CH_3 -phenanthrene (4) may be understandable if an additional molecular motion of

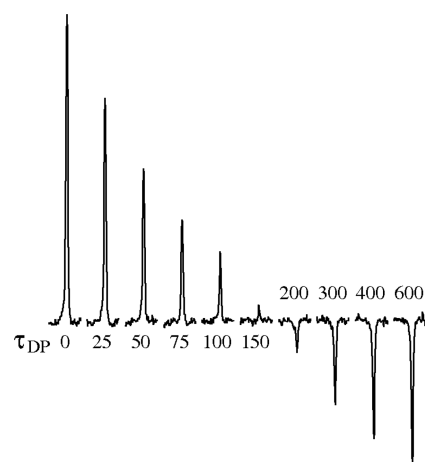


Figure 3. $^{13}\text{C}\{^1\text{H}\}$ CP/DP MAS experiments for the CH_3 group in 4-methylphenanthrene (4). Each of the CP/DP experiments used 512 scans, a contact time of $2000 \mu\text{s}$, a relaxation delay of 4.0 s , and a MAS frequency of $\nu_r = 3.0 \text{ kHz}$. The DP time (τ_{DP}) is in μs . The ZCT for the CH_3 group is observed at $163 \pm 5 \mu\text{s}$.

the complete, almost planar phenanthrene ring makes a small contribution to the overall dynamics for the CH₃ group.

Finally, for comparison with the ¹³C{¹H} CP/DP MAS NMR ZCT for a few simple organic molecules containing proposed/possible congested CH₃ groups, but also *additional* motional axis other than a *single* CH₃-X rotational axis, we also performed ¹³C CP/DP experiments for hexamethylbenzene (HMB)¹⁶ (9) (which most likely exhibits an additional motional contribution from planar rotations of the benzene ring) and sodium 3-trimethylsilylpropylsulfonate (10) (often referred to as “the solid-state TMS-salt”). ¹³C{¹H} CP/DP MAS NMR experiments for (9) and (10) are displayed in Figures 1S and 2S of the Supporting Information. The corresponding ZCTs for (9) (300 ± 20 μs) and (10) (540 ± 25 μs) are summarized in Table 1 along with the ZCTs (*vide supra*) for samples (1), (7), and (4).

Table 1. Zero-Crossing (ZC) Times Determined from Cross-Polarization/Depolarization (CP/DP) Experiments for Samples: (1) ¹³CH₃-Si≡/HO-Si≡; (7) L-Alanine; (4) 4-CH₃-phenanthrene; (9) Hexamethylbenzene (HMB); (10) Sodium 3-Trimethylsilylpropylsulfonate Including Error Limits^a

samples	(1)	(7)	(4)	(9)	(10)
ZC times (μs)	120 ± 3	120 ± 5	162 ± 5	300 ± 20	540 ± 25

^aThe experiments for (1), (7), and (4) are presented in the present article, while the experiments for (9) hexamethylbenzene (HMB) and (10) sodium 3-trimethylsilyl-propylsulfonate are shown in the Supporting Information.

With only little knowledge of the structure for the ¹³CH₄ reaction product (1),¹ apart from the one-bond ¹³CH₃-Si≡ and HO-Si≡ covalent bonds for the units in a helical or chain silicate structure, the identity of the ZCTs of 120 μs for (1) and the CH₃ group of L-alanine (7) immediately turned our attention to the very precise crystal and molecular structure determined for L-alanine from neutron diffraction.¹⁶ Calculations in that study¹⁶ show that the barrier to rotation for the CH₃ group in L-alanine (7) is estimated to be 5.6 ± 1.1 kcal/mol (i.e., 23.4 ± 4.6 kJ/mol) and that for the NH₃⁺ group is 20 ± 7 kcal/mol (i.e., 84 ± 29 kJ/mol). In addition, it was observed that “The L-alanine molecules are linked together by hydrogen bonds to form a three-dimensional network and that the methyl groups are situated in channels formed by this network”.¹⁶ This structure is in accordance with the favored structure we recently proposed for a helical silicate structure as opposed to a chain structure for the ¹³CH₃-Si≡/HO-Si≡ reaction product (1).¹ To obtain further insight into the geometry and structure of the channels formed by the hydrogen-bonded molecular three-dimensional network from the L-alanine molecules, Figure 4 shows a drawing of the channel structure, looking down the crystallographic *c*-axes, perpendicular to the plane of the paper based on the neutron diffraction structure.¹⁶ Figure 4a displays the complete structure for one particular *a*-*b* plane of six L-alanine molecules perpendicular to the *c*-axes and further illustrates the positions of the two neighboring CH₃ groups near the center of the channel. In Figure 4b, the CH₃ groups have been removed from all six L-alanine molecules in order to better envisage the channel and its dimensions (illustrated here by the “potato-like” brown space).

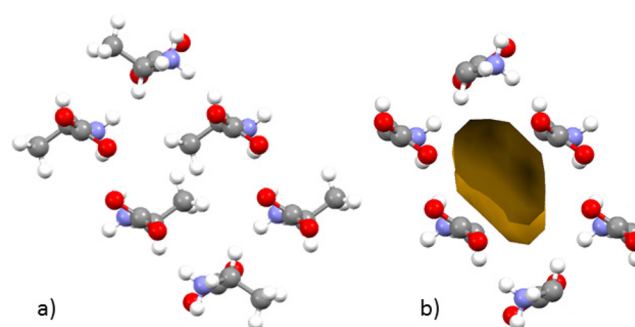


Figure 4. Display of part of the neutron diffraction crystal and molecular structure for L-alanine (according to Lehmann et al.¹⁶). (a) Looking down the *c*-axis and illustrating the complete crystal structures of the six L-alanine molecules in a *a*-*b* plane which form part of the hydrogen-bonded network forming the channels hosting the CH₃ groups. As shown here with two CH₃ groups near the center of the plane for the six molecules. (b) By removal of all six CH₃ groups from the molecular structure in (a) this display serves to illustrate the space and geometry of the channel structure formed by the hydrogen-bonded framework of the L-alanine molecules.

Following the structural investigation for L-alanine (7),¹⁶ an experimental solid-state VT static ²H NMR spin-lattice relaxation study of polycrystalline CD₃-L-alanine (8) by Batchelder et al.¹⁷ resulted in determination of an activation energy of 22.6 kJ/mol for the CD₃ group rotational 3-site jump process. This experimental value is in good agreement with the estimated value of 23.4 kJ/mol¹⁶ (*vide supra*) reported about 10 years earlier in the neutron diffraction study¹⁶ and in good agreement with the experimental value 20.0 kJ/mol determined for CD₃-L-alanine (8) from VT static ²H line shape analysis by Griffin and co-workers.¹⁹

Low-Temperature VT ²H MAS NMR Experiments of CD₃ Groups in 4-CD₃-Phenanthrene (5/6) and the CD₃-Si≡/DO-Si≡ (2) Material. “4-CD₃-phenanthrene” Sample. As pointed out in the Experimental Section, while the synthesis of ordinary 4-CH₃-phenanthrene (4) results in an extremely pure product, the synthesis of 4-CD₃-phenanthrene (5) turned out to be identified as an ~1:1 mixture of 4-CD₃-phenanthrene (5) and its isotopomer 4-CD₂H-3D-phenanthrene (6) according to liquid-state ¹³C and ¹H NMR (*vide supra*). Thus, the two different ²H NMR resonances observed in this study for the solid-state VT experiments for this sample refer to the single CD₃ resonance (~3.0 ppm) in 4-CD₃-phenanthrene (5) along with an overlay of the two different resonances for the CD₂H-group (~3.0 ppm) and the aromatic 3D-phenanthrene resonance (~7.7 ppm) in 4-CD₂H-3D-phenanthrene (6). We note that the MAS condition of $\nu_r = 6.0$ kHz employed in the VT ²H MAS experiments did not allow resolution of the CD₃- and CD₂H-group resonances for the two isotopomers in the ²H MAS spectra but on the positive side apparently reduced the broadening effect of ²H-¹H dipolar coupling in the observed ²H MAS spectra.

The low-temperature VT ²H MAS spectra of the (5/6) isotopomeric “4-CD₃-phenanthrene” sample were conducted at eight different temperatures in the range starting from -170 to -30 °C with an increase of 20 °C between each experiment. Figure 5 displays three experimental spectra which show the most prominent changes in appearance for the “CD₃/CD₂H groups only” in this temperature range, i.e., at the lowest (-170 °C) region, center (-90 °C) region, and highest temperature (-30 °C) region. Another noteworthy observation from these

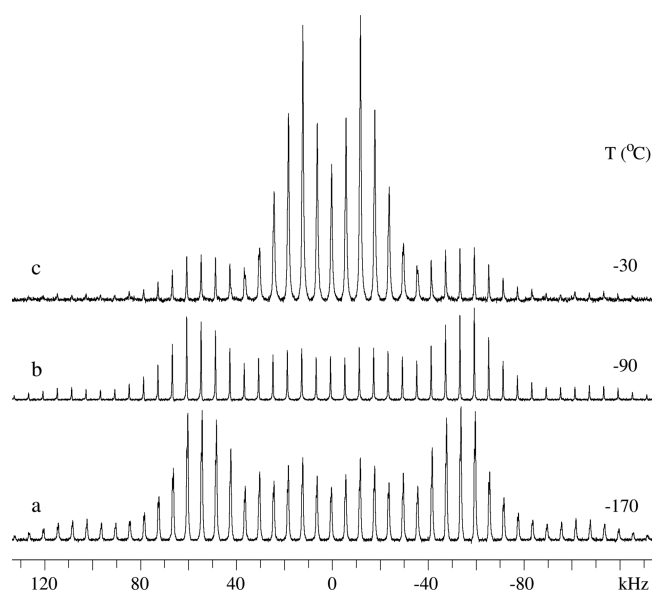


Figure 5. Selected low-temperature ^2H VT MAS NMR spectra for the three temperatures which show the most predominant changes in spectral appearances for the “ $\text{CD}_3/\text{CD}_2\text{H}$ groups only” for the total of eight temperatures for the (5/6) isotopomeric “4- CD_3 -phenanthrene” sample. (a) Spectrum at -170 °C. (b) Spectrum at -90 °C showing the 3D-phenanthrene part “only” of the $\sim 50\%$ for the 4- CD_2H -3D-phenanthrene (6) sample. (c) Spectrum at -30 °C. Analysis and optimized fitting of horizontal expansions for these three spectra are presented in Figures 3S–5S of the Supporting Information. See also the text and Table 2.

three spectra is that the resonance at ~ 3.0 ppm for the $\text{CD}_3/\text{CD}_2\text{H}$ groups gets nulled in the center temperature region. This is in accordance with previous simulations for such dynamic experiments.^{20,21} Finally, we also took advantage of the three experimental spectra shown in Figure 5 for determinations of the different ^2H quadrupole coupling parameters, i.e., in the slow regime $k(\text{CD}_3/\text{CD}_2\text{H}) \ll C_Q$ at -170 °C, in the fast regime $k(\text{CD}_3/\text{CD}_2\text{H}) \gg C_Q$ at -30 °C, and for the aromatic 3D deuteron in 4- CD_2H -3D-phenanthrene (6) at -90 °C by optimized fitting of simulated to the experimental spectra. Comparisons of horizontal expansions for these three experimental and their optimized simulated spectra are illustrated in Figures 3S–5S of the Supporting Information, while the corresponding spectral parameters are listed in Table 2.

To further illustrate the spectral changes in more detail occurring during the low-temperature VT ^2H MAS experiments for the studied temperature range, Figure 6 shows a series of six selected horizontal expansions out of the total of eight acquired low-temperature spectra. These six expansions display the centerband for the complete spectrum at highest frequency ~ 0 kHz (~ 0 ppm) followed by the first four spinning sidebands (ssbs) in the low-frequency spectral region from -4 to -24 kHz. The expansions clearly show the appearance, disappearance, and reappearance of the low-frequency resonance at ~ 3.0 ppm for the $\text{CD}_3/\text{CD}_2\text{H}$ resonance in both the centerband and ssbs, which occurs in going from the lowest to the highest temperature in the studied temperature range.

Therefore, to retrieve the optimum dynamic data from the acquired low-temperature VT ^2H MAS spectra, the single resonance ^2H MAS spectrum for the aromatic 3D deuteron in 4- CD_2H -3D-phenanthrene (6) (observed at -90 °C in Figures

Table 2. ^2H Quadrupole Coupling Parameters (C_Q , η_Q) and Isotopic Chemical Shifts (δ_{iso}) Determined from Low-Temperature VT ^2H MAS NMR Spectra at -170 , -93 , and -30 °C Shown in Figure 5 and Figures 3S–5S for the (5/6) Isotopomeric “4- CD_3 -phenanthrene” Sample Obtained at 92.12 MHz (14.1 T)^a

expt temp; Figures	sites	C_Q (kHz)	η_Q	δ_{iso} (ppm)
-170 °C; Figures 5a and 3S	CD_3 ; 3.9	171.4	0.0	3.00
-170 °C; Figures 5a and 3S	C3-D; 1	180.6	0.0	7.73
-90 °C; Figures 5b and 4S	C3-D; 1	179.3	0.0	7.70
-30 °C; Figures 5c and 5S	CD_3 ; 3.7	52.3	0.0	3.00
-30 °C; Figures 5c and 5S	C3-D; 1	175.3	0.0	7.67

^aThe column “sites” shows the relative intensity ratio for the $\text{CD}_3/\text{CD}_2\text{H}$ resonance at 3.0 ppm versus the C3-D resonance at ~ 7.7 ppm for the (5/6) isotopomeric “4- CD_3 -phenanthrene” sample constituting a mixture of $\sim 50\%$ of 4- CD_3 -phenanthrene (5) and $\sim 50\%$ of 4- CD_2H -3D-phenanthrene (6) as obtained from the optimized STARS fits to the experimental spectra. The intensity ratios were not performed in a quantitative manner because of the huge variation of the $T_1(^2\text{H})$ relaxation times with temperature. Thus, the intensity of the C3-D resonance has been fixed to 1 for all three spectra. If recorded under fully $T_1(^2\text{H})$ relaxed conditions, an intensity ratio of 5:1 would be expected for the $\text{CD}_3/\text{CD}_2\text{H}$ versus the C3-D intensities for the spectra at -170 and -30 °C. The experimental error for $\delta_{\text{iso}}(^2\text{H})$ is about ± 0.5 ppm, while the precision for the chemical shift differences between the two groups of resonances is about ± 0.2 ppm. The precision for the determined $C_Q(^2\text{H})$ quadrupole coupling constants is ± 2 kHz for the C_Q values >170 kHz and ± 1 kHz for $C_Q \sim 52$ kHz.

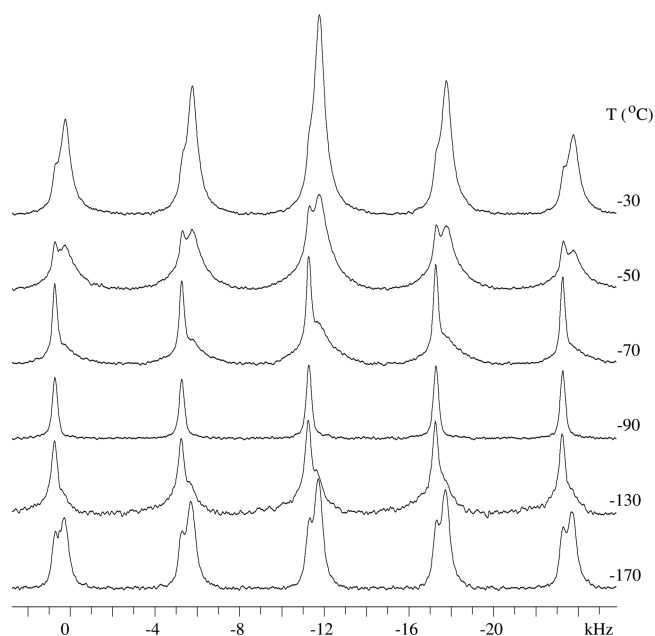


Figure 6. Six selected expansions display the centerband of the complete spectrum at highest frequency ~ 0 kHz (to the left), followed by the first four spinning sidebands (ssbs) in the low-frequency spectral region from -4 to -24 kHz for the (5/6) isotopomeric “4- CD_3 -phenanthrene” sample in the temperature range -170 to -30 °C (see text for further information).

5b and 6) has been subtracted from all eight ^2H MAS spectra acquired in the temperature range from -170 to -30 °C. This resulted in the elimination of the disturbing aromatic 3D resonance from 4- CD_2H -3D-phenanthrene (6) in the eight experimental VT ^2H MAS spectra for this temperature range. These are shown in the column to the right in Figure 7, which

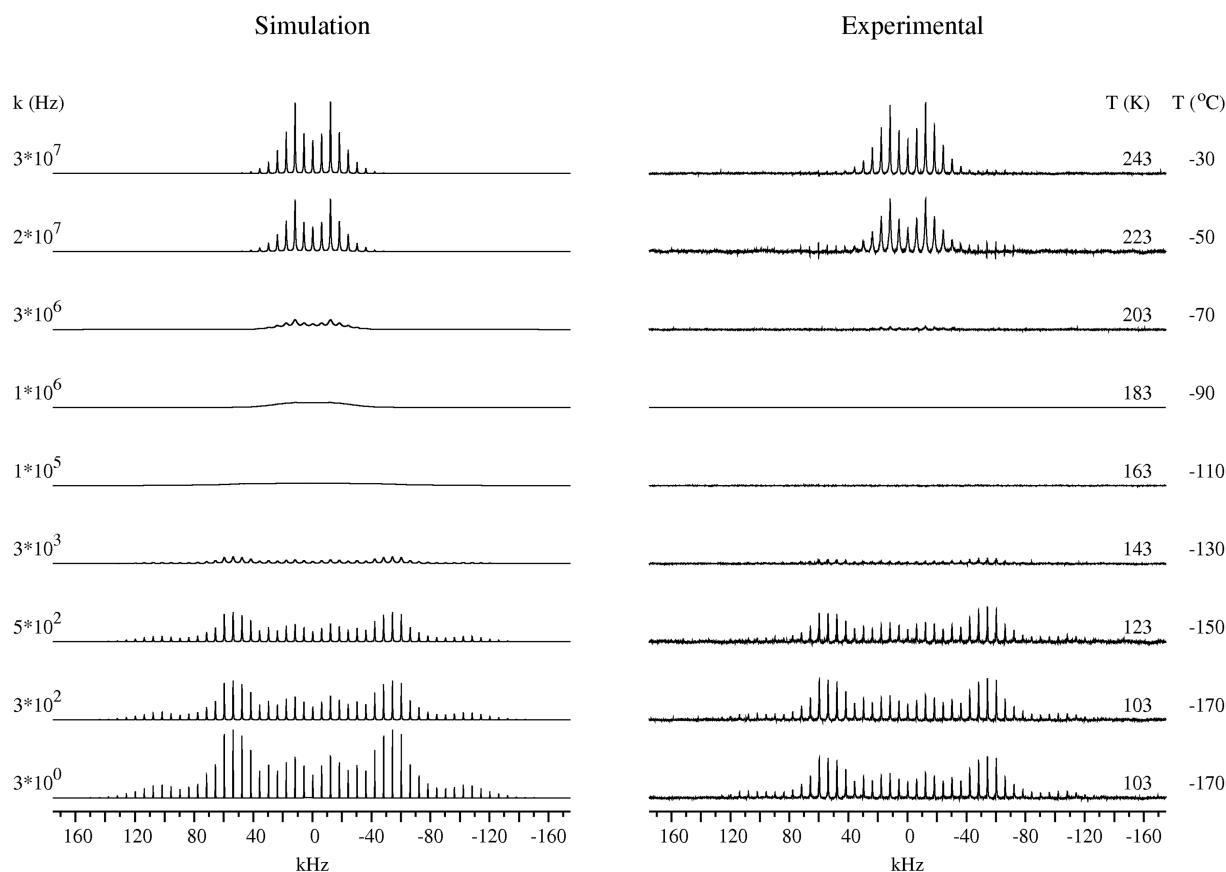


Figure 7. Low-temperature “CD₃/CD₂H-only” experimental ²H VT MAS NMR spectra (after subtraction of the 3D-phenanthrene “only” spectrum at 7.70 ppm; see Figure 5b, Figure 4S, and Figure 6 at –90 °C) for the 4-CD₂H-3D-phenanthrene (6) sample from all experimental spectra of the CD₃ group dynamics. Experimental spectra (right) and simulations (left).

displays the upper eight “clean” CD₃/CD₂H resonance evolution of the VT ²H MAS spectra from –170 to –30 °C, followed by an additional identical display of the –170 °C spectrum at the bottom for relaxation illustration purposes (*vide infra*). The first upper eight experimental and simulated spectra, along with their corresponding rate constants k for the 3-site jumps of the methyl groups were used to perform a first preliminary Arrhenius plot of $\ln(k)$ versus $10^3/T$ (K), according to a first-order reaction $k = A \times \exp(-E_a/RT)$ or $\ln(k) = (-E_a/R) \times (1/T) + \ln(A)$. This resulted in an acceptable linear fit for the upper seven temperatures (>-170 °C), while the rate constant $\ln(k)$ for the number eight value at –170 °C turned out to fall way outside the optimized linear plot including all eight k -values. Thus, it was decided to conduct a second and final Arrhenius linear fit of $\ln(k)$ versus $10^3/T$ (K) using only the first seven upper $\ln(k)$ temperature values (>-170 °C). The Arrhenius linear fit for this seven-point fit is shown in Figure 8. In addition to the seven-point fit in Figure 8, we have introduced two extra points in this figure at the temperature $10^3/T$ (K) = 9.7 corresponding to –170 °C. The point marked in blue at $\ln(k) = 5.7$ corresponds to the experimental spectrum evaluated from simulations based on intensity/line width, while the point marked in red is an artificial point corresponding to the linear fit and to $\ln(k) = 1.1$ (or $k = 3 \times 10^0$). The simulated spectrum corresponding to $k = 3 \times 10^0$, shown to the left of the experimental spectrum, exhibits a somewhat narrower line width (longer T_2) and increased height compared to the simulations performed for the higher temperature spectra. These observations are all in

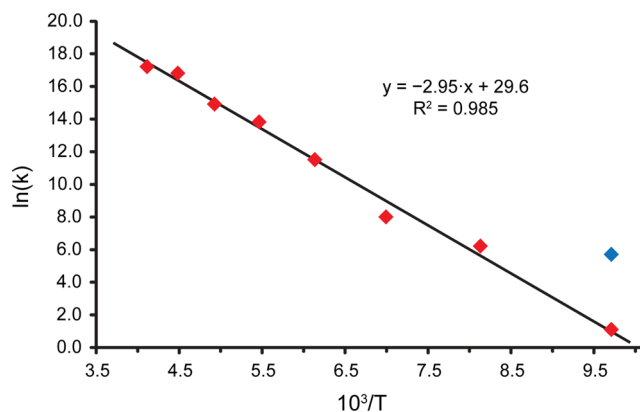


Figure 8. Determination of the activation energy E_a as obtained from the plot of $\ln k$ versus $1/T$ ($1/K$). $E_a = 24.5 \pm 1.5$ kJ/mol and $A = 29.6 \pm 1.0$.

accordance with the highly increased T_1 relaxation time experienced at –170 °C and thus a partly saturation of the spectrum observed employing the experimental conditions to acquire the spectrum at this low temperature (*vide supra*).

The excellent fit and correlation for the upper seven temperatures/data points presented in Figure 7 result in a barrier for the 3-site jumps for the CD₃/CD₂H groups in the (6/7) isotopomeric “4-CD₃-phenanthrene” sample of $E_a = 24.5 \pm 1.4$ kJ/mol along with a value for the corresponding frequency factor $A = 7.2 \times 10^{12}$. This solid-state E_a value is somewhat higher compared to the original experimental

literature value ($E_a = 21.1$ kJ/mol; no error limits reported) determined from liquid-state 4-CH₃-phenanthrene (4) employing ¹H relaxation studies.¹⁸ According to the comprehensive solid-state ²H NMR spin–lattice relaxation study on amino acids and peptides by Batchelder et al.,¹⁷ the difference between the methyl-group reorientation activation energies determined by ¹H and ²H NMR in previous and their own study may result from different crystal packings of optically active and racemic forms. Obviously, this could also lead to the slightly different ¹H liquid-state and ²H solid-state NMR activation energy results observed here for 4-methylphenanthrene.

In addition, we also point out that the value $E_a = 24.5 \pm 1.4$ kJ/mol determined here for the solid-state “4-CD₃-phenanthrene” sample is only slightly higher than the value $E_a = 22.6$ kJ/mol (no error limits reported) determined experimentally for polycrystalline CD₃-L-alanine (8) by Batchelder et al.¹⁷ from a solid-state VT static ²H NMR spin–lattice relaxation study. Therefore, it appears that 4-methylphenanthrene, originally investigated employing ¹H liquid-state $T_1(^1\text{H})$ relaxation by Takagoshi et al.,¹⁸ still has a marginal lead with respect to exhibiting the highest methyl-group 3-site jump activation energy compared to its L-alanine competitor according to the present solid-state ²H NMR experiments.

Furthermore, in addition to the advantages of employing solid-state ²H NMR experiments for determination of CD₃ group 3-site jump activation energies, it may also serve as a sensitive probe for the CD₃ molecular geometry employing ²H quadrupolar coupling constants (C_Q) or quadrupolar splittings ($\Delta\nu_q$) for an undistorted axially symmetric ($\eta_Q = 0$) powder pattern, i.e., $\Delta\nu_q = C_Q/1.5$. Thus, it was tempting to apply the approach by Batchelder et al.¹⁷ to our data in order to evaluate a possible geometric change for the CD₃ molecular geometry within the “4-CD₃-phenanthrene” sample from ideal tetrahedral geometry. Thus, for $C_Q = 171.4$ kHz at -170 °C (Table 2) we have $\Delta\nu_q = 114.3$ kHz, and using the expression for the averaged quadrupolar splitting $\bar{\Delta\nu}_q = \Delta\nu_q \times S$, where $S = (3 \cos^2 \theta - 1)/2$ and θ is the angle between the C–D bond and the 3-fold axis, we are able to calculate the averaged quadrupolar splitting $\bar{\Delta\nu}_q$ for small variations in θ . (Note: θ denotes the angle used by Batchelder et al.¹⁷ and is identical to the angle named β_{PC} by Larsen.²¹) For an ideal tetrahedron (tetrahedral angle of 109.47°), $\theta = 70.53^\circ$ and $S = 1/3$, and we calculate $\bar{\Delta\nu}_q = 114.3 \times 1/3 = 38.10$ kHz while for the experimental value $C_Q = 52.3$ kHz at -30 °C (Table 2) we observe $\bar{\Delta\nu}_q = 34.9$ kHz. Thus, using the observed value of $\bar{\Delta\nu}_q = 34.9$ kHz in a back-calculation of θ , we obtain $\theta = 68.89^\circ$, which is only about 1.64° off the ideal tetrahedral geometry. We point out that the θ -value derived at for CD₃-L-alanine (8) by Batchelder et al.,¹⁷ $\theta = 68.75^\circ$, is only marginally lower than obtained here for the sample. Since the introduction of this approach by Batchelder et al.,¹⁷ their explanation that the discrepancy between calculated and observed averaged $\Delta\nu_q$ values is mainly due to the methyl group geometry slightly deviates from exact tetrahedral geometry, a fact that has been generally accepted by the scientific community. For example, the angle θ has been introduced as the variable parameter β_{PC} in Larsen’s software programs^{20,21} in order to improve the optimization of the simulated to the experimental spectra. Thus, we note that independent of the above calculated θ value ($\theta = 68.89^\circ$) for “4-CD₃-phenanthrene”, the eight simulated spectra in Figure 7, conducted using Larsen’s software, have independently employed a noniterative, but “by-eye” optimized value $\beta_{PC} = 68 \pm 1^\circ$, a value in good agreement with the above

calculated value. Accordingly, this approximate θ -value could turn out to be a benchmark indicating a heavily congested CD₃ group but clearly has to await future experiments along these lines. We note that similar distortions from exact tetrahedral geometry for congested CH₃ groups have earlier been reported for L-alanine (7) in the neutron diffraction study of the crystal structure¹⁶ and for hexamethylbenzene.¹⁶

CD₃–Si≡/DO–Si≡ Material or Sample (2). The -170 °C low-temperature ²H MAS NMR spectrum of sample (2), i.e., the first low-temperature ²H MAS spectrum for this sample (*vide supra*), is shown in Figure 9. We note that this sample is

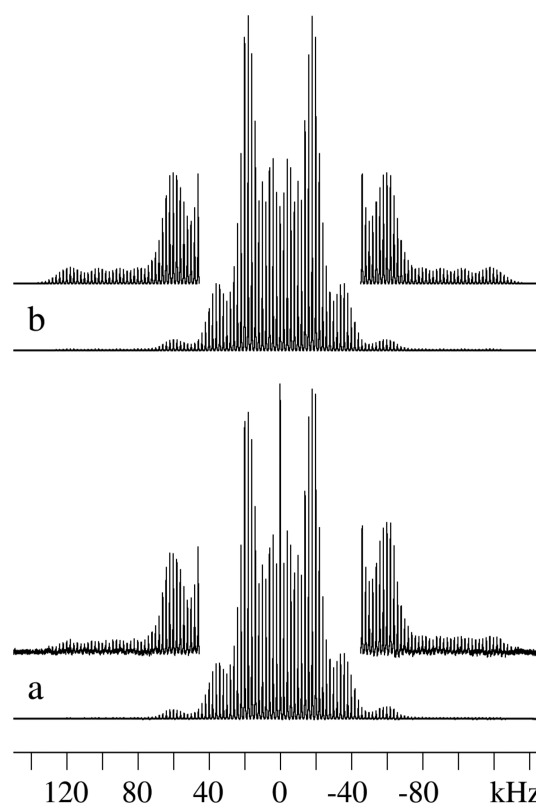


Figure 9. Low-temperature (-170 °C) experimental and simulated ²H MAS NMR spectra recorded at 92.12 MHz (14.1 T) of a $< 100 \mu\text{m}$ sieved sample for the reaction product (2) (¹³CD₄ + SiO₂ + Simax flask; open air) described in ref 1. (a) Experimental spectrum using a 3.2 mm o.d. rotor, $\nu_r = 2.0$ kHz, 65 536 scans, and a relaxation delay of 0.1 s (i.e., a total spectrometer time of ~ 1.8 h). The two insets above the standard display of the spectrum show the outer wings for the DO–²⁹Si≡ site with a vertical expansion by a factor 12 relative to the standard display. (b) Simulated fitted ²H MAS spectrum (STARS) with variations of all spectral parameters (C_Q , η_Q , δ_{iso}) for the two CD₃–Si≡ and DO–Si≡ sites and including the relative intensity for these sites (see Table 3).

the reaction product (CD₄ + SiO₂ + Simax flask; $< 100 \mu\text{m}$ sieved sample in open air).¹ The appearance of the spectrum in Figure 9 shows up as a great surprise for two reasons: (i) The spectrum acquired at -170 °C (Figure 9) is identical to the spectrum obtained at RT for the same sample as presented in Figure 6 of ref 1. For example, see Table 3 which compares the (C_Q , η_Q) spectral parameters determined for the spectrum in Figure 9 with those reported for the RT spectrum in Table 1 of ref 1. The second reason (ii) is that the relaxation delay used in the acquisition of the -170 °C ²H MAS spectrum (Figure 9) could be reduced to just 0.1 s without the CD₃ resonance in the

Table 3. ^2H Quadrupole Coupling Parameters (C_Q , η_Q) and Isotropic Chemical Shifts (δ_{iso}) Determined from the Low-Temperature VT ^2H MAS NMR Spectrum at -170 °C of the $\text{CD}_3\text{-Si}\equiv$ and $\text{DO-Si}\equiv$ Sites Shown in Figure 9 for the Reaction Product ($^{13}\text{CD}_4 + \text{SiO}_2 + \text{Simax Flask}$; See Figure 9 Caption); Corresponding Parameters Determined at RT (Ref 1, Table 1) Are Shown for Comparison of the Parameters at the Two Widely Different Temperatures^a

expt temp; Figure	sites	C_Q (kHz)	η_Q	δ_{iso} (ppm)
-170 °C; Figure 9a	CD_3 ; 3.0	57.9	0.09	0.19
-170 °C; Figure 9a	OD; 0.40	173.2	0.06	0.53
RT; Figure 6a, ref 1	CD_3 ; 3.0	56.5	0.06	0.03
RT; Figure 6a, ref 1	OD; 0.27	170.1	0.01	0.35

^aThe column “sites” shows the relative intensity ratio for the CD_3 and OD resonances as obtained from the optimized STARS fits to the experimental spectra, by assuming an intensity of 3 for the CD_3 resonance and accordingly adjusting the intensity for the OD resonance. The somewhat too low intensity obtained for the OD resonance compared to an expected “ideal” intensity ratio of 3:1 may result from a combination of (i) deuterium–hydrogen exchange caused by handling the sample in an open air atmosphere and (ii) partial saturation of the OD resonances caused by the experimental conditions (e.g., too short relaxation delays employed to acquire the presented spectra). The experimental errors for the spectral parameters are $C_Q(\text{CD}_3)$ and $C_Q(\text{OD}) \pm 0.5$ and ± 1.5 kHz, respectively; $\eta_Q \pm 0.05$; $\delta_{\text{iso}}(^2\text{H}) \pm 0.5$ ppm, while the precision for the chemical shift differences $\Delta\delta_{\text{iso}}(^2\text{H})$ between the two groups of resonances is only ± 0.1 ppm.

spectrum showing any sign of saturation. As discussed above in the section on the “4- CD_3 -phenanthrene sample”, this indicates that at -170 °C we are nowhere even close to freezing-out the expected 3-site jump process for the CD_3 group in the $\text{CD}_3\text{-Si}\equiv/\text{DO-Si}\equiv$ material (2). As discussed and expected (*vide supra*), based on the identical and very short CP/DP ZCT of 120 μs for the two fully protonated samples $\text{CH}_3\text{-Si}\equiv/\text{HO-Si}\equiv$ (1) and L-alanine (7) along with a 3-site jump activation energy $E_a \sim 22 \pm 2$ kJ/mol determined in the two independent studies of $\text{CD}_3\text{-L-alanine}$ (8) by Batchelder et al.¹⁷ and Griffin and co-workers,¹⁹ it was an unexpected surprise to observe no indication of a spectral change at -170 °C for the $\text{CD}_3\text{-Si}\equiv/\text{DO-Si}\equiv$ material (2). Furthermore, combined with an observed decrease for the distribution of E_a values ~ 16 kJ/mol with a spread of ~ 6 kJ/mol for CD_3 groups in some proteins^{24,25} in the temperature range 85–140 K and a simultaneous increase in T_1 values by about 2 orders of magnitude at the lower end of this temperature range led us to study the channel and helix structures in more details for L-alanine (7) and the silicate $\text{CH}_3\text{-Si}\equiv/\text{HO-Si}\equiv$ material (1) because they were proposed as important structures in the recent investigation.¹

The strongly hydrogen-bonded three-dimensional molecular framework in L-alanine, elucidated by neutron diffraction¹⁶ and earlier by X-ray diffraction,³⁰ forms channels along the crystal structure c -axis. These channels contain the methyl groups in a severely constraint situation as illustrated in Figure 4a. The activation energy studies on $\text{CD}_3\text{-L-alanine}$ (8) by Batchelder et al.¹⁷ and Griffin and co-workers¹⁹ (*vide supra*) are in full agreement with the constraint methyl groups observed in these structural investigations, as is the very short CP/DP ZCT of 120 μs for the methyl group in L-alanine (7) determined in this work. To seek some additional information on the constrained space experienced by the methyl groups in L-alanine (7), we

have taken advantage of Figure 4b with the CH_3 groups removed to measure the distance (across the brown “potato”) between the two carbon atoms displaced slightly above and below the a - b plane, respectively, and which carry the two CH_3 groups on opposite side of the channel. We measured this distance to be 5.63 Å. In addition, from Figure 4a we also measured the distance between the two C atoms within the two same methyl groups across the channel from both the neutron structure (3.681 Å)¹⁶ and X-ray structure (3.68 Å).³⁰ Considering the high similarity for the neutron and X-ray diffraction structures used and compared here, these distances are identical and also identical to the quote by Batchelder et al.:¹⁷ “The 3.6-Å methyl–methyl intermolecular distance in the crystal,³⁰ 0.4 Å less than the van der Waals diameter of the methyl group, apparently imposes severe restrictions on methyl reorientation.” Thus, we assume that the proposed/estimated van der Waals diameter of ~ 4 Å by Batchelder et al.¹⁷ for a methyl group is based on a summation of van der Waals radii according to the van der Waals diameter being $= 2 \times r(\text{C-H}) + r(\text{C-C}) = 2 \times 1.2 + 1.7 = 4.1$ Å. This information on the much smaller measured distance of 5.63 and ~ 8 Å for the approximate channel diameter incorporating the alternate opposite positions of two fairly large CH_3 groups from L-alanine (7) constitute useful information in a comparison with the diameter size of the helical versus chain silicate structure determined for the free radical silicate intermediate (originally studied by EPR¹) following its reaction with $^{13}\text{CO}_2$ (*vide infra*).¹ While many of the early EPR investigations employed different irradiation methods for the production of this free radical silicate intermediate in Pyrex or quartz glasses, they were unable to distinguish between a silicate chain or a helical structure for this intriguing specimen. It was first with the identification of $^{13}\text{CO}_2$ being encapsulated in the reaction product between the $^{13}\text{CO}_2$ gas and the free radical silicate intermediate based on the typical ^{13}C chemical shift anisotropy (CSA) spinning sideband (ssb) pattern (see Figure 9 in ref 1) that a helical structure appeared as evidence for this free radical submicroscopic (nanomaterial) silicate glass structure (or at least for the reaction product).

Evidence for this conclusion is mainly based on a few recent studies^{26,27} involving dynamics of $^{13}\text{CO}_2$ molecules confined in micropores of solids studied by solid-state ^{13}C NMR. In particular, we have looked into the approach used by Omi et al.,²⁶ who analyzed the observed axially symmetric ^{13}C CSA tensor for the $^{13}\text{CO}_2$ molecules in their static ^{13}C NMR spectra of an activated carbon fiber (ACF) powder material. In their study, shortly described here for the reader to follow their strategy, the authors compared their results with those determined earlier for bulk solid $^{13}\text{CO}_2$ ($\Delta = -222$ ppm).³¹ The two principal values characterizing their axially symmetric ^{13}C CSA tensor, $\delta_{\parallel} = \delta_{zz} = -33$ ppm and $\delta_{\perp} = \delta_{xx} = \delta_{yy} = 178$ ppm were determined from simulation of the experimental spectrum obtained at RT. Using our standard convention for the chemical shift anisotropy (δ_{σ}) as outlined in eqs 2–4, and used in the STARS simulation software,²⁹ we obtain $\delta_{\sigma} = 140$ ppm, which considering the opposite sign of the direction for the δ - and σ (Δ)-scale equals the values $\bar{\Delta} = -140$ ppm and $\bar{\delta}_{\sigma} = 140$ ppm. The most interesting point now, following the agreement on the two definitions of chemical shift anisotropy, is that “The value of $\bar{\Delta} = -140$ ppm is somewhat smaller than that of bulk solid CO_2 ($\Delta = -222$ ppm).³¹ This indicates that CO_2 molecules strongly adsorbed in the ACF micropores are not rigid like solid CO_2 . ^{13}C chemical shift anisotropy is

averaged by rapid and anisotropic molecular motion." Thus, this molecular motion is assumed to consist of an uniaxial rotation of the CO₂ molecules around an axis tilted by a certain angle from the molecular CO₂ axis. Following the author's²⁶ approach of comparison their partly averaged value $\bar{\Delta} = -140$ ppm with that for bulk solid CO₂ ($\Delta = -222$ ppm) value,³¹ and using the equation³²

$$\bar{\Delta}/\Delta = (3 \cos^2 \beta_{PC} - 1 - \eta \sin^2 \beta_{PC} \cos 2\alpha_P)/2 \quad (5)$$

finally lead to the conclusion that their static sample is performing rapid and anisotropic rotation around an axis, tilted $\sim 30^\circ$ away from the molecular CO₂ axis.²⁶

For a cylindrical molecule, as e.g. the CO₂ spy molecule, of length = l , diameter $d = 2r$, and the anisotropic rotation axis tilted by ν° from the molecular axis, it requires a cylindrical channel with radius = R , where R is given by

$$R = l/2 \sin(\nu) + r \cos(\nu) \quad (6)$$

for the molecular precession to take place. For the size of the CO₂ molecule with $l = 0.54$ nm, $r = 0.17$ nm, and $\nu = 30^\circ$, it requires a cylindrical channel with a diameter of at least $D = 2R = 0.564$ nm (5.64 Å) for the molecular precession to take place. Interestingly, without making any detailed structural comparisons, this channel diameter appears identical to the value of 5.63 Å we measured for the channel diameter of CH₃-L-alanine (7) (*vide infra*) in Figure 4b. Alternatively, considering the molecular size of the CO₂ molecule as a cylinder capped with half a ball at each end and with a total length $l = 0.54$ nm (including two ball radii $2r = 0.34$ nm), we obtain a corresponding cylindrical channel diameter $D = 2R$ for

$$R = (l - 2r)/2 \sin(\nu) + r \quad (7)$$

For the same anisotropic rotation axis tilted by $\nu = 30^\circ$ from the CO₂ molecular axis, we arrive at a cylindrical channel diameter/space of at least $D = 2R = 0.44$ nm (4.4 Å) for the molecular precession to take place. This value is similar to the value of 0.42 nm derived by Omi et al.²⁶

Following these intriguing results, it was decided to investigate if we could take advantage of the encapsulated ¹³C CO₂ molecules in the silicate sample (3) (i.e., ¹³C CO₂-tumbled SiO₂ grains-Simax flask; sieved, <250 μm, and handled in open air) as a possible spy (molecular probe) to provide insight into the channel structure and/or any dynamic behavior of the encapsulated CO₂ molecules based on the ¹³C CSA parameters determined at RT (25 °C) using ¹³C MAS NMR (see Figure 9 in ref 1). These parameters are $\delta_\sigma = 187$ ppm, $\eta_\sigma = 0.22$, and $\delta_{iso} = 125.4$ ppm. Using eqs 2–4 (*vide supra*), we now convert these parameters into their principal axis values. But before we do so, we note that the small value $\eta_\sigma = 0.22$ is about the size of its experimental error (~ -0.20), i.e., corresponding to an almost axially symmetric CSA tensor. Thus, in accordance with CO₂ being a linear molecule, we assume that $\eta_\sigma = 0$ (axially symmetric tensor, which requires only two principal values for its full characterization), and in the following conversion this leads to $\delta_{||} = \delta_{zz} = -62$ ppm, $\delta_{\perp} = \delta_{xx} = \delta_{yy} = 219$ ppm, $\delta_{iso} = 125$ ppm, and $\delta_\sigma = 187$ ppm (or $\bar{\Delta} = -187$ ppm).

Now, employing the equation³² $\bar{\Delta}/\Delta = (3 \cos^2 \beta_{PC} - 1 - \eta \sin^2 \beta_{PC} \cos 2\alpha_P)/2$ (*vide supra*), we arrive at $\bar{\Delta}/\Delta = 187/222 = (3 \cos^2 \beta_{PC} - 1)/2$ after substitution of the appropriate values, which leads to $\beta_{PC} = 19^\circ$ (or 161°). Thus, the shape of the ¹³C MAS NMR spectrum (Figure 9¹) appears as arising from MAS rotation of rigid CO₂ molecules constituting part of the sample.

It is noteworthy, however, that in contrast to the static ¹³C NMR spectra obtained by Omi et al.²⁶ and shown in Figure 5,²⁶ our ¹³C MAS NMR spectrum (Figure 9¹) exhibits no observable ¹³C singlet resonance in the region ~ 125 ppm attributable to highly mobile ¹³CO₂ molecules. In addition to the regions for the encapsulated CO₂ molecules, this shows that no other parts/regions of the sample contribute to the ssb intensity pattern in the observed ¹³C MAS NMR spectrum. This is most likely due to the way this sample/reaction product was handled/opened at RT in the standard atmosphere following its reaction.¹ Anyway, the spectrum shape has been analyzed based on the change in the value for β_{PC} , i.e., = 19° , as shown above. Thus, from the ratio $\bar{\Delta}/\Delta = 188/222$ it appears that the observed MAS spectrum arises from rotation along an axis which is tilted 19° from the linear ¹³CO₂ molecular axis. Using the cylinder only as well as the ball-capped cylinder as shapes for the CO₂ molecule, the dimensions for CO₂ used above, and a tilt of $\nu = 19^\circ$ for the linear CO₂ axis with respect to the rotation axis, we obtain the following approximate minimum channel diameters for the CO₂ molecule rotate considering the present experimental parameters: 5.0 Å (cylinder only) and 4.1 Å (ball-capped cylinder).

From these experiments on the encapsulated CO₂ molecules in sample (3), we estimate that the minimum channel diameter required to accommodate the rotating linear ¹³CO₂ molecules, however, tilted relative to the rotation axis for the silicate reaction product for sample (3) is in the range ~ 4.0 – 5.0 Å. For decades this is the first evidence of a possible helical as opposed to a chain silicate structure for this intriguing silicate Si free-radical intermediate and/or some of its reaction products. However, for the present case of its reaction with CO₂ the formation of helices induced by the polar linear ¹³CO₂ molecules from a chain structure cannot be excluded.

CONCLUSIONS

This study shows that the "zero-cross time" (ZCT) observed during the depolarization period in solid-state ¹³C{¹H} cross-polarization/depolarization (CP/DP) MAS experiments may serve to indicate the presence of CH₃ groups residing in highly congested environments. Early variable temperature (VT) dynamic studies of methyl group 3-site jump barriers show that the CD₃ group in CD₃-L-alanine (crystalline powder) and CH₃ group in 4-CH₃-phenanthrene (solution) exhibit the highest barriers observed for methyl group 3-site jumps (~ 20 – 25 kJ/mol) observed so far. The corresponding ZCTs determined in the present solid-state study for CH₃-L-alanine (120 μs) and 4-CH₃-phenanthrene (162 μs) are the shortest ZCTs observed for CH₃ groups. In addition to the earlier reported solution-state 3-site jump barrier for 4-CH₃-phenanthrene (21.1 kJ/mol), the present study determines the corresponding solid-state CD₃-jump barrier for 4-CD₃-phenanthrene (24.5 kJ/mol) employing VT ²H MAS NMR experiments for the first time for such measurements.

A clue to unravel the unknown structure of the reaction product between the free-radical silicate nanomaterial and CH₄ (shown to contain both one-bond ¹³CH₃-Si≡ and HO-Si≡ covalent bonds) is the determination of a ZCT = 120 μs, a value exactly identical to that determined for CH₃-L-alanine. For that reason the "channel" structure formed by the strongly hydrogen-bonded molecular CH₃-L-alanine entities has been evaluated. Thus, the approximate channel diameter of 5.6 Å for L-alanine led us to propose a helical structure of similar diameter for the ¹³CH₃-Si≡/HO-Si≡ nanomaterial of the

reaction product. Early EPR studies were unable to distinguish between a helical and chain structure for the free-radical silicate material itself. Moreover, the helical structure proposed here for the $^{13}\text{CH}_3\text{-Si}\equiv\text{HO-Si}\equiv$ reaction product is supported by the CO_2 -encapsulated silicate helical structure with a diameter in the range $\sim 4.0\text{--}5.0\text{ \AA}$, as also reported here.

In contrast to the helical structure suggested for the $^{13}\text{CH}_3\text{-Si}\equiv\text{HO-Si}\equiv$ material from the present experimental results, the corresponding deuterium isotopomeric $\text{CD}_3\text{-Si}\equiv\text{DO-Si}\equiv$ material, obtained as the reaction product between the free-radical silicate and CD_4 , exhibits a structural change from helical to an open chain $\text{CD}_3\text{-silicate}$ structure. This structural change is based on the results of the present low-temperature ^2H MAS NMR experiments. To our knowledge, this appears to be the first reported example of a structural change induced by substitution of ^2H for ^1H in a compound at least studied by NMR spectroscopy.

Finally, it is emphasized that cautious use of the CP/DP experiment for determination of ZCTs may serve as a useful tool in studies of congested methyl groups.

■ ASSOCIATED CONTENT

Supporting Information

The Supporting Information is available free of charge on the ACS Publications website at DOI: 10.1021/acs.jpcc.7b08826.

ZCT experiments of some partly constrained organics, experimental and simulated low-temperature ^2H MAS NMR spectra of deuterated 4-methylphenanthrene (PDF)

■ AUTHOR INFORMATION

Corresponding Author

*(H.J.J.) Tel +45 8715 5332; Fax +45 8619 6199; e-mail hja@chem.au.dk

ORCID

Hans J. Jakobsen: 0000-0002-9530-495X

Anders T. Lindhardt: 0000-0001-8941-4899

Jorgen Skibsted: 0000-0003-1534-4466

Notes

The authors declare no competing financial interest.

■ ACKNOWLEDGMENTS

This work results from a collaborative research program between Aarhus University and the NHMFL, with H.J.J. being a Visiting Professor at the NHMFL (MagLab), Florida State University (FSU), Tallahassee, in the period 2012–2017. The authors acknowledge support of the “Mars Group”, Aarhus University for the use of the tumbling apparatus in the preparation of several gas–solid reaction products. Thanks to Dr. Jacob Overgaard, Department of Chemistry, Aarhus University, for fruitful discussions on the crystal structure of L-alanine and for calculations of the hydrogen-bonded channel structure formed by the L-alanine molecules. The solid-state $^{13}\text{C}\{^1\text{H}\}$ CP/DP MAS NMR experiments were performed at the Department of Chemistry, Aarhus University. The low-temperature ^2H MAS NMR experiments were all performed at the NHMFL, which is supported by National Science Foundation Cooperative Agreement DMR-1157490, the State of Florida, and the U.S. Department of Energy.

■ REFERENCES

- (1) Jakobsen, H. J.; Song, L.; Gan, Z.; Hung, I.; Bildsøe, H.; Skibsted, J.; Bak, E.; Finster, K.; Nørnberg, P.; Jensen, S. K. J. NMR and EPR Studies of Free-Radical Intermediates from Experiments Mimicking the Winds on Mars: A Sink for Methane and Other Gasses. *J. Phys. Chem. C* **2016**, *120*, 26138–26149.
- (2) Jensen, S. J. K.; Skibsted, J.; Jakobsen, H. J.; ten Kate, I. L.; Gunnlaugsson, H. P.; Merrison, J. P.; Finster, K.; Bak, E.; Iversen, J. J.; Kondrup, J. C.; Nørnberg, P. A Sink for Methane on Mars? The Answer is blowing in the Wind. *Icarus* **2014**, *236*, 24–27.
- (3) Brown, G. An ESR Study of Electron and Hole Trapping in Gamma-Irradiated Pyrex. *J. Mater. Sci.* **1975**, *10*, 1841–1848.
- (4) Brown, G.; Ammar, E. A. E.; Thorp, J. S. Q-Band ESR of γ -Irradiated Pyrex. *J. Mater. Sci.* **1976**, *11*, 1775–1776.
- (5) Lee, S.; Bray, P. J. Electron Spin Resonance Studies of Irradiated Glasses Containing Boron. *J. Chem. Phys.* **1963**, *39*, 2863–2873.
- (6) Griscom, D. L.; Taylor, P. C.; Ware, D. A.; Bray, P. J. ESR Studies of Lithium Borate Glasses and Compounds γ Irradiated at 77 K: Evidence for a New Interpretation of the Trapped-Hole Centers Associated with Boron. *J. Chem. Phys.* **1968**, *48*, 5158–5173.
- (7) Taylor, P. C.; Griscom, D. L. Toward a Unified Interpretation of ESR Trapped Hole-Centers in Irradiated Borate Compounds and Glasses. *J. Chem. Phys.* **1971**, *55*, 3610–3611.
- (8) Weeks, R. A. Paramagnetic Resonance of Lattice Defects in Irradiated Quartz. *J. Appl. Phys.* **1956**, *27*, 1376–1381.
- (9) Weeks, R. A.; Nelson, C. M. Irradiation Effects and Short-Range Order in Fused Silica and Quartz. *J. Appl. Phys.* **1960**, *31*, 1555–1558.
- (10) Silsbee, R. H. Electron Spin Resonance in Neutron-Irradiated Quartz. *J. Appl. Phys.* **1961**, *32*, 1459–1462.
- (11) Webster, C. R.; Mahaffy, P. R.; Atreya, S. K.; Flesch, G. J.; Farley, K. A.; et al. (i.e., MSL Science Team) Low Upper Limit to Methane Abundance on Mars. *Science* **2013**, *342*, 355–357.
- (12) Webster, C. R.; Mahaffy, P. R.; Atreya, S. K.; Flesch, G. J.; Mischna, M. A.; Meslin, P.-Y.; Farley, K. A.; Conrad, P. G.; Christensen, L. E.; Pavlov, A. A.; et al. Methane Detection and Variability at Gale Crater. *Science* **2015**, *347*, 415–417.
- (13) Melchior, M. T. “22nd Experimental NMR Conference,” Asilomar, California, Poster B-29, 1981.
- (14) Wu, X.; Zilm, K. W. Complete Spectral Editing in CPMAS NMR. *J. Magn. Reson., Ser. A* **1993**, *102*, 205–213.
- (15) Sangill, R.; Rastrup-Andersen, N.; Bildsøe, H.; Jakobsen, H. J.; Nielsen, N. C. Optimized Spectral Editing of ^{13}C MAS NMR Spectra of Rigid Solids Using Cross-Polarization Methods. *J. Magn. Reson., Ser. A* **1994**, *107*, 67–78.
- (16) Lehmann, M. S.; Koetzle, T. F.; Hamilton, W. C. Precision Neutron Diffraction Structure Determination of Protein and Nucleic Acid Components. I. The Crystal and Molecular Structure of the Amino Acid L-Alanine. *J. Am. Chem. Soc.* **1972**, *94*, 2657–2660.
- (17) Batchelder, L. S.; Niu, C. H.; Torchia, D. A. Methyl Reorientation in Polycrystalline Amino Acids and Peptides: A ^2H NMR Spin-Lattice Relaxation Study. *J. Am. Chem. Soc.* **1983**, *105*, 2228–2231.
- (18) Takegoshi, K.; Imashiro, F.; Terao, T.; Saika, A. ^1H and ^{13}C NMR Study on Rotation of Congested Methyl Groups in Methyl Substituted Phenanthrenes, Fluorenes, and Fluorenones. *J. Chem. Phys.* **1984**, *80*, 1089–1094.
- (19) Beshah, K.; Olejniczak, E. T.; Griffin, R. G. Deuterium NMR Study of Methyl Group Dynamics in L-Alanine. *J. Chem. Phys.* **1987**, *86*, 4730–4736.
- (20) Larsen, F. H. Simulations of Molecular Dynamics in Solid-State NMR Spectra of Spin-1 Nuclei Including Effects of CSA- and EFG-Terms Up to Second Order. *Solid State Nucl. Magn. Reson.* **2007**, *31*, 100–114.
- (21) Larsen, F. H. Simulation of Molecular Motion of Quadrupolar Nuclei in Solid-State NMR Spectra. In *Annual Reports on NMR Spectroscopy*; Webb, G. A., Ed.; Academic Press: Burlington, 2010; Vol. 71, pp 103–137.
- (22) Larsen, F. H.; Jakobsen, H. J.; Ellis, P. D.; Nielsen, N. C. Sensitivity-Enhanced Quadrupolar-Echo NMR of Half-Integer Quad-

rupolar Nuclei. Magnitudes and Relative Orientation of Chemical Shielding and Quadrupolar Coupling Tensors. *J. Phys. Chem. A* **1997**, *101*, 8597–8606.

(23) Larsen, F. H.; Jakobsen, H. J.; Ellis, P. D.; Nielsen, N. C. Molecular Dynamics from ^2H Quadrupolar Carr-Purcell-Meiboom-Gill Solid-State NMR Spectroscopy. *Chem. Phys. Lett.* **1998**, *292*, 467–473.

(24) Vugmeyster, L.; Ostrovsky, D.; Moses, M.; Ford, J. J.; Lipton, A. S.; Hoatson, G. L.; Vold, R. L. Comparative Dynamics of Leucine Methyl Groups in Fmoc-Leucine and in a Protein Hydrophobic Core Probed by Solid-State Deuteron Nuclear Magnetic Resonance over 7–324 K Temperature Range. *J. Phys. Chem. B* **2010**, *114*, 15799–15807.

(25) Vugmeyster, L.; Ostrovsky, D.; Lipton, A. S. Origin of Abrupt Rise in Deuteron NMR Longitudinal Relaxation Times of Protein Methyl Groups below 90 K. *J. Phys. Chem. B* **2013**, *117*, 6129–6137.

(26) Omi, H.; Ueda, T.; Miyakubo, K.; Eguchi, T. Dynamics of CO_2 Molecules Confined in the Micropores of Solids as Studied by ^{13}C NMR. *Appl. Surf. Sci.* **2005**, *252*, 660–667.

(27) Moore, J. K.; Sakwa-Novak, M. A.; Chaikittisilp, W.; Mehta, A. K.; Conradi, M. S.; Jones, C. W.; Hayes, S. E. Characterization of a Mixture of CO_2 Adsorption Products in Hyperbranched Aminosilica Adsorbents by ^{13}C Solid-State NMR. *Environ. Sci. Technol.* **2015**, *49*, 13684–13691.

(28) Bielecki, A.; Burum, D. P. Temperature Dependence of ^{207}Pb MAS Spectra of Solid Lead Nitrate. An Accurate, Sensitive Thermometer for Variable-Temperature MAS. *J. Magn. Reson., Ser. A* **1995**, *116*, 215–220.

(29) Bildsøe, H. Varian Manual, STARS (SpecTrum Analysis of Rotating Solids) User's Guide, Publication No 87–195233–00, Rev. A0296, 1996; based on Jakobsen, H. J.; Skibsted, J.; Bildsøe, H.; Nielsen, N. C. Magic-Angle Spinning NMR Spectra of Satellite Transitions for Quadrupolar Nuclei in Solids. *J. Magn. Reson.* **1989**, *85*, 173–180.

(30) Simpson, H. J.; Marsh, R. E. The Crystal Structure of L-Alanine. *Acta Crystallogr.* **1966**, *20*, 550–555.

(31) Beeler, A. J.; Orendt, A. M.; Grant, D. M.; Cutts, P. W.; Michl, J.; Zilm, K. W.; Downing, J. W.; Facelli, J. C.; Schindler, M. S.; Kutzelnigg, W. Low-Temperature ^{13}C Magnetic Resonance in Solids. 3. Linear and Pseudolinear Molecules. *J. Am. Chem. Soc.* **1984**, *106*, 7672–7676.

(32) Schmidt-Rohr, K.; Spiess, H. W. *Multidimensional Solid-State NMR and Polymers*; Academic Press: London, 1994.